Topological models of 2D cellular structure. II. z=5

1991 J. Phys. A: Math. Gen. 24 4655

(http://iopscience.iop.org/0305-4470/24/19/026)

J. Phys. A: Math. Gen. 24 (1991) 4655-4675. Printed in the UK

Topological models of 2D cellular structures: II. $z \geqslant 5$

G Le Caër

Laboratoire de Science et Génie des Matériaux Métalliques, associé au CNRS, URA 159, Ecole des Mines, F-54042 Nancy-Cedex, France

Received 28 March 1991, in final form 24 June 1991

Abstract. Topological models of 2D cellular structures are associated with planar tessellations with topologically unstable sites which belong to $z > 3$ polygons. This degeneracy is removed by replacing every z-vertex by $z-3$ added sides. A method which uses the diagonal triangulation of the dual tiling is also described. The number of stable configurations, called states, is enumerated and various distributions which characterize these states are calculated as a function of z. Topological properties of the associated cellular structures are derived for a distribution of equiprobable and independent states on the various sites and for z ranging from 5 to infinity. The distributions $P(n)$ of the number n of cell sides for the latter distribution of states are typical of the $P(n)$ of planar cuts of polycrystals and differ from the $P(n)$ of soap froths. Deviations from the Aboav-Weaire relation, which describes the correlations between nearest-neighbour cells, occur mainly for $n = 3$ and $n > 9$.

1. Introduction

In a previous paper (Le Caër 1991, referred to hereafter as I) we described a method for constructing topological models of cellular structures and we applied it to 2D structures. The models are topological as they only yield the relative repartition of cells and do not need or provide information about angles and edge lengths. The method is based on lattices with topologically unstable sites, which belong to more than z_s polygons ($z_s = 3$ in 2D), and on rules which allow removal of this degeneracy. For every value of the vertex coordination number (or valence) z (z-vertex) and for a given rule, there are $Q(z)$ stable arrangements, called states, built from 3-vertices only. Cellular models are associated with distributions of states on the lattice sites.

In paper I, the stable configurations are obtained by replacing every z-vertex by $z-3$ sides (Thompson 1917, chapter 8, figure 158, Almgren and Taylor 1976, and I). In that case, the set of states is closed with respect to neighbour switching (I) which is one of the two basic topological transformations in 2D cellular structures (Weaire and Rivier 1984, table 1). As the chosen rule does not create or annihilate cells, a cell of the topological cellular model is associated with every polygon of the lattice. Every state is characterized by a z-dimensional vector $\boldsymbol{S}_k$ ($k = 1, \ldots, Q(z)$), whose components S_{kj} ($j = 1, \ldots, z$) have values in the range from 1 to $z-2$. S_{kj} is the number of vertices that polygon number j will have at the considered lattice site in the final stable arrangement (figure 1). Some constraints on the components are described in appendix 1. The state components allow us to calculate the number n of sides of the cell (n-cell) and define its neighbours (appendix 1): n is the sum of the S_{kj} values

0305-4470/91/194655+21$03.50

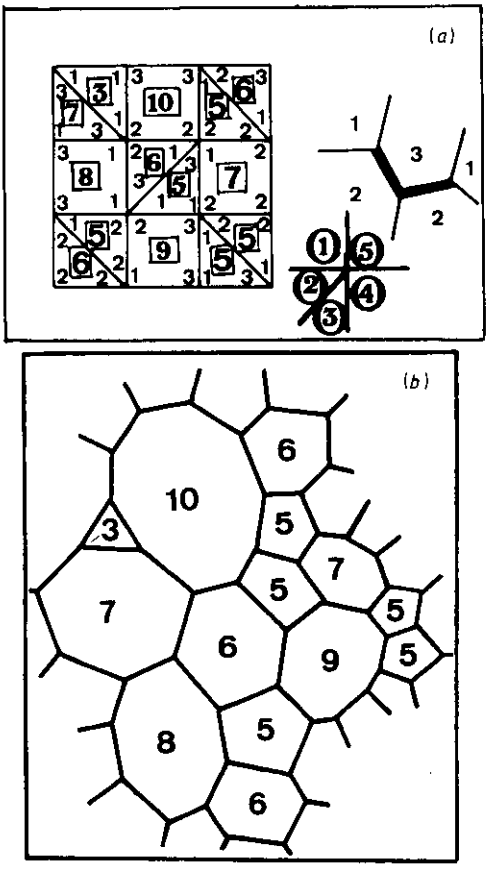

Figure 1. Examples of distributions of states for: (*a*) $z = 5$, with the numbering convention (circled numbers) and values of the number n of cell sides (boxed numbers) obtained by summing up the S_{kj} values inside the corresponding squares and triangles. Stable configurations have been drawn: bold lines represent the added cell sides. (*b*) A cellular structure consistent with the distribution of states of (*a*).

which are inside the subject lattice polygon (figure 1). It is therefore unnecessary to perform the transformation to the stable cellular structure in order to investigate its topological properties and full profit can be taken from the use of a periodic lattice. As the stable structure at the subject lattice site consists of $z-2$ trivalent vertices, the sum

$$T_k = \sum_{j=1}^{z} S_{kj} = 3z - 6 \tag{1}$$

is independent of the state: all vectors $\boldsymbol{V}_k = \boldsymbol{S}_k - (3z-6)\boldsymbol{D}_1/z$, where $\boldsymbol{D}_1 = (1, 1, 1, \ldots, 1)$, belong to a hyperplane perpendicular to $\boldsymbol{D}_1$. A 'configuration' $\{\boldsymbol{S}_k\}$ has been defined in paper I as the subset of states whose component values (S_{kj}) coincide by a circular permutation in the positive sense of rotation. We need to find in the set of states all states deduced from any of them by circular permutations, in both senses of rotation, as required by the statistical equivalence of all z polygons at any vertex. As a consequence, the set of component values S_{kj} for a fixed j is the same for all j.

For example, $Q(7) = 42$ with $1 \leqslant S_{kj} \leqslant 5$ and six configurations are obtained:

[{1512222}] [{1223124}, {1322142}]

[{1231314}, {1313214}] [{1232133}].

The second and third, fourth and fifth configurations respectively are exchanged by a circular permutation in the negative sense of rotation while the first and the sixth are invariant by such a permutation. It is therefore better, in contrast to paper I, to define a configuration $[\boldsymbol{S}_k]$ by using the circular permutation in both senses of rotation. For a fixed value of j (from 1 to 7), there are 14, 14, 9, 4 and 1 component values of 1, 2, 3, 4 and 5 respectively among the 42 possible values of S_{kj}.

Topological characterizations of cellular structures usually include the determination of the distribution of cell sides $P(n)$ and of the n-dependence of the mean number $m_n(1)$ of sides of the first neighbour cells of n-cells. The Aboav-Weaire law (Aboav 1970, 1980, Weaire 1974), expresses that $m_n(1)$ is linearly related to $1/n$ by

$$m_n(1) = 6 - a + (6a + \mu_2)/n \tag{2}$$

where μ_2 is the variance of the distribution of n: $\mu_2 = \langle n^2 \rangle - \langle n \rangle^2$, with $\langle n \rangle = 6$ as a consequence of Euler's relation in 2D (Weaire and Rivier 1984) and $\langle n m_n(1) \rangle = \mu_2 + 36$ (Weaire 1974). In many natural random cellular structures, the parameter a is of the order of 1.2 (Aboav 1980).

The case of the square lattice or of any lattice topologically equivalent to it ($z = 4$) has been discussed in detail in paper I. The model has been observed to account reasonably for some experimental or simulation results ($4 \leqslant n \leqslant 8$, $Q(4) = 2$) for a distribution of independent states at every lattice site with a single parameter, the probability p of finding one given state at any site. Agreement with other experimental results not quoted in paper I for $z = 4$ may be of interest: the model ($p = 0.831$) gives a very reasonable account of the topological properties of the cellular domain patterns in magnetic garnet films for a zero bias field (Babcock *et al* 1990). The main differences from the latter experiment results are that $P(4)$ is predicted to be 0.02 instead of zero and that the calculated $m_n(1)$ are systematically larger than the experimental ones but by only 1% on the average. For independent states on a square lattice, the best least-squares fit of the theoretical $nm_n(1)$ to the $nm_n(1)$ values calculated from equation (2) gives $a[nm_n] = 1.5$, for all p (D Fraser, personal communication), while a direct fit of $m_n(1)$ with equation (2) gives $a[m_n]$ which depends on p (equation (10) of paper I). These differences arise from an n^2 weighting of the first method with respect to the second. If $m_n(1)$ does not follow the Aboav-Weaire relation exactly, significantly different values of 'a' may be obtained from different least-square fits to the data (section 3.2, see also Fraser 1991).

Only preliminary results were given for $z \geqslant 5$. In order to study the variability of their topological properties, in the present paper we shall study the cellular structures which result from a distribution of equiprobable and independent states (called DIES) on the vertices of various regular or quasiregular tessellations with z from 5 to infinity. In section 2, we establish the expressions which allow the calculation of $Q(z)$ and the distribution $P_0(i, z)$ ($i = 1, \ldots, z-2$) of the S_{kj} values for a fixed j as a function of z. In section 3, we obtain the side distribution $P(n)$ and $m_n(1)$ for the previous structures. The validity of the Aboav-Weaire law is discussed. In section 4, the derived distributions are compared with the $P(n)$ calculated by various authors to model cellular structures and their growth and with experimental results obtained from planar cuts of polycrystals and from soap froths. A possible link between models and actual structures is discussed.

2. Enumeration of states

Every added side is connected at least to one added side for $z > 4$ (figure 1) and the associated graph is a connected graph without cycles, that is a tree (Berge 1970, Essam and Fisher 1970). The number of states $Q(z)$ is the number of configurations of added sides with their z incoming sides (figure 1). The graph associated with any state has z monovalent external vertices and $z-2$ trivalent internal vertices as all states are structurally stable. The states can be constructed by taking all possible planted trivalent trees or binary trees with $z-2$ internal vertices (Knuth 1973, Viennot 1990). As described by Gardner (1976) and by Cohen (1978), the construction of planted trivalent trees is related to Euler's polygon-triangulation problem which searches for the number of ways by which a fixed convex polygon can be divided into triangles by non-intersecting diagonals (diagonal triangulation, Cohen 1978, appendix 1). The number of planted trivalent trees with $z-2$ internal vertices is given by a Catalan number C_{z-2} (equation (3), Knuth 1973, Gardner 1976, Cohen 1978, Viennot 1990):

$$Q(z) = C_{z-2} = C_{2z-4}^{z-2}/(z-1). \tag{3}$$

When $z \to \infty$, the number of states $Q(z)$ is well approximated by $Q(z) \approx 4^z/\{\pi^{1/2} z^{3/2}\}$ (Knuth 1973). $Q(z)$ increases exponentially, being 2, 5, 14, 16 796 and 0.5774×10^{56} for $z = 4$, 5, 6, 12 and 100 respectively. Binary trees have recently been used by Vannimenus and Viennot (1989) to analyse tree-like patterns in physics, such as 2D diffusion-limited aggregation patterns. The case of equiprobable states corresponds to the 'random binary tree' for which all possible binary trees are considered with the same weight (Vannimenus and Viennot 1989).

We will derive equation (3) by a different method which enables us to calculate $P_0(i, z)$, the distribution of $i = S_{kj}$ ($k = 1, \ldots, Q(z)$, $i = 1, \ldots, z-2$) for a fixed j which may take any value in the range $1, \ldots, z$. $P_0(i, z)$ does not depend on j. River networks containing no lakes, islands or junctions of more than two streams may also be represented by planted trivalent trees (Shreve 1966, 1967, Moon 1980, Viennot 1990). A network may be obtained here by considering any state and by choosing any external vertex as the outlet. Shreve (1967) has associated a round trip with every network: one starts at the outlet and traverses the network always turning left at internal vertices and reversing directions at external vertices, until the outlet is again reached. A sequence of $I = +1$ and $E = -1$ is generated by recording an I the first time a given internal vertex is traversed and an E the first time a given external vertex is traversed (figure 2(a)). The sequence is composed of $(z-2)$ I and of $(z-1)$ E (as no E are associated with the outlet). All walks begin with an I and end with two successive E. Moreover, the partial sums s_i obtained by summing up all the $+1$ and -1 collected up to step i since the start of the walk can never be negative except at the last step where the sum is -1 (Shreve 1967, figure 2(b)). A similar walk, found by Lukasiewicz, in which a worm crawls up the trunk and around the entire tree, is also described by Gardner (1976). This walk may equally be considered as a 1D random walk with a reflecting barrier. An example is represented graphically in figure 2(b), starting from the origin O ($x = 0$, $y = 0$), going to (1, 1) for $i = 1$, and finishing at F ($x = 2z-3$, $y = 1$). There are C_{z-2} (equation 3) paths such that $s_1 \geqslant 0, \ldots, s_{2z-5} \geqslant 0$ among the C_{2z-4}^{z-2} paths joining the origin to the point $2(z-2)$ of the x-axis (Feller 1957, theorem 2, p 71, Cohen 1978, p 37).

In order to calculate $P_0(i, z) = n(i, z)/Q(z)$, we only need to consider the paths which begin with a sequence of $iI(+1)$ values followed by one $E(-1)$ at least ($S_{kl} =$

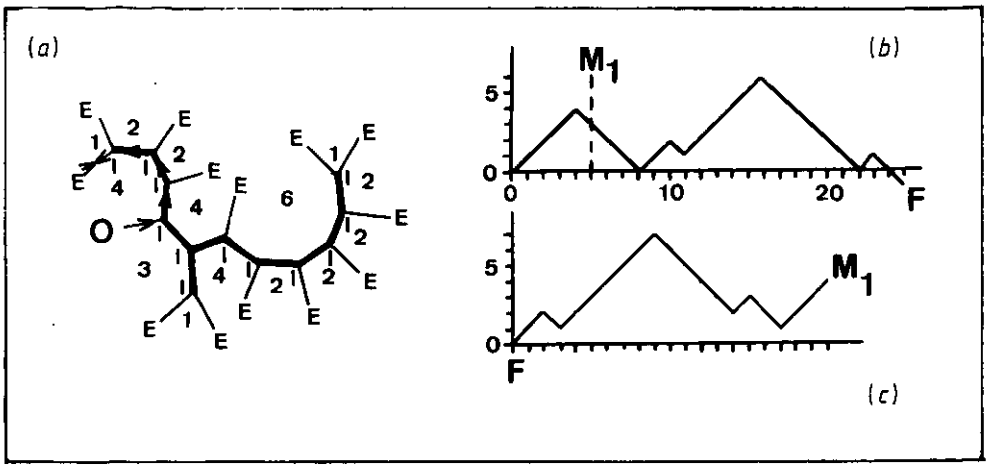

Figure 2. (*a*) An example of a state for $z=14$ (inspired by figure 1 of Shreve 1967). O indicates the chosen outlet. Arrows have been drawn from O to the first external vertex reached during the round trip. (*b*) The path from O to F associated with the round trip of (*a*). (*c*) The reversed path from F to M_1 obtained from (*b*).

$i, M_1, x_1=i+1, y_1=i-1$) (figure 2(*b*)). It is identical to calculate the number $n(i,z)$ of reversed paths, starting at the end F taken as the origin ($x'=0, y'=0$) and finishing at M_1 ($x_1'=2z-4-i, y_1'=i$) with the conditions $s_1'>0, \ldots, s_{2z-4-i}'>0$ (figure 2(*c*)). The number of paths is

$$n(i,z)=\{i/(z-2)\}C_{2z-5-i}^{z-3} \tag{4}$$

(Feller 1957, the ballot theorem p 70, Cohen 1978, p 38). There may be more than one path from O to M_1 as one can insert the E at various positions in the series of I. With any of these paths from O to M_1 are associated $n(i,z)$ paths from M_1 to F. This explains simply why $n(1,z)=n(2,z)$ as all states whose first component is $S_{k1}=1$ are associated with paths beginning with the sequence IEI ($s_3>0$) while those for which $S_{k1}=2$ give rise to the sequence IIE; M_1 is identical for both cases. Combining equations (3) and (4), we finally write $P_0(i,z)$ in a form convenient for computer calculations ($z>3$, $P_0(1,3)=1$):

$$\begin{aligned} &P_0(1,z)=P_0(2,z)=(z-1)/(4z-10) \\ &P_0(i,z)=P_0(1,z)\{i/2^G\}\prod_{k=2}^{i-G}[(z-1-G-k)/(2z-3-2k)] \end{aligned} \tag{5}$$

where $G=[i/2]$ is the integral part of $i/2$ and $i\geqslant 3$. When $z\to\infty$, we obtain the result quoted in paper I:

$$P_0(i,\infty)=i/2^{i+1}. \tag{6}$$

As $P_0(1,z)=P_0(2,z)$, $P(4)=3P(3)$ for a DIES on the vertices of any triangular tessellation.

The conditional distributions $P_{|L|}(j|i,z)$, which is the probability of finding a component $S_{km+L}=i$ knowing that $S_{km}=j$ for a given and fixed m ($k=1,\ldots,Q(z)$), are helpful in order to calculate $m_n(1)$. The distribution $P_{|L|}$ does not depend on m ($=1,\ldots,z$), L varies from $-[z/2]$ to $[z/2]$, while $m+L$ is defined on a circle and

ranges from 1 to z. For $L=1$, we consider all states with a first component $S_{k1}=j$ and a second component $S_{k2}=i$. The associated paths begin with the sequence $I\ldots IEI\ldots IE$ where the first sequence of I has a length j and the second one a length $(i-1)$. Using reversed paths, as before, from F, as the origin, to $(x'=2z-4-i-j,\ y'=i+j-2)$ we calculate the number $n_1(j|i,z)$ of paths ($z\geqslant 4$):

$$n_1(j|i,z)=\{(i+j-2)/(z-3)\}C_{2z-5-i-j}^{z-4} \tag{7}$$

and

$$P_1(j|i,z)=n_1(j|i,z)/n(j,z) \tag{8}$$

where $n(j,z)$ is given by equation (4). The latter distribution takes a simple form for $j=1,2$:

$$P_1(1|i,z)=P_0(i-1,z-1) \qquad P_1(2|i,z)=P_0(i,z-1). \tag{9}$$

The previous relations give, as expected,

$$P_1(1|1,z)=0 \qquad P_1(z-2|i,z)=\partial_{i1}. \tag{10}$$

A similar calculation gives $P_2(1|i,z)=P_0(i,z-1)$ (appendix 2). When $z\to\infty$, $P_1(2|i,\infty)=P_2(1|i,\infty)=P_0(i,\infty)$ which means an absence of correlations between component 2 and its first neighbours and between component 1 and its second neighbours. The coefficient of correlation Π of the bivariate distribution

$$P_b(j,i,z)=P_1(j|i,z)P_0(j,z)$$

is negative: $\Pi=-(z+6)/(4z-6)$.

We associate with any distribution of states a distribution $F_0(i,z)$ $(i=1,\ldots,z-2)$ which gives the fraction of component values $S(m,j)$ which are equal to i, averaged over all lattice sites (labelled by m) and over all z polygons at every z-vertex:

$$F_0(i,z)=\lim_{N\to\infty}\left\{\sum_{m=1}^{N}\sum_{j=1}^{z}\partial[S(m,j)-i]/(Nz)\right\}. \tag{11}$$

For $z\leqslant 5$, $F_0(i,z)=P_0(i,z)$, as there exists only one configuration for such valences: [111], [1212], [12213] for $z=3$, 4 and 5 respectively. We deduce from equation (1) that

$$\langle i\rangle=\mathrm{av}(z,0)=\sum_{i=1}^{z-2} iF_0(i,z)=(3z-6)/z. \tag{12}$$

Relation (12) holds for any distribution of states as it holds for every state at every lattice site. It is a consequence of Euler's relation in 2D, which requires that $\langle n\rangle=6$, as it contributes to the sum which gives the total mean number of sides. Expressions involving the ratio $(z-2)/z$ are frequently met in the study of tilings (Grünbaum and Shephard 1987). Equations (11) and (12) are easily generalized to lattices which include vertices with different valences. The average $\langle i(j,z,1)\rangle$ of the distribution $P_1(j|i,z)$ is $(1\leqslant j\leqslant z-2)$:

$$\langle i(j,z,1)\rangle=\mathrm{av}(j,z,1)=[(j+1)/j]\{(2z-j-4)/(z-1)\}. \tag{13}$$

This relation, consistent with the negative value of Π, helps to explain why few-sided cells have many-sided neighbouring cells. Complementary results about the previous distributions are given in appendix 2. Section 3 is devoted to the calculation of $P(n)$ and of $m_n(1)$ for $z\geqslant 5$ and to the application of equations (5)–(13) for large values of z.

3. Tessellations with $z \geqslant 5$

3.1. $z = 5$

Figure 1(a) shows a lattice with $z = 5$ ($Q(5) = 5$) which is topologically equivalent to a basic net occurring in complex alloy structures (Frank and Kasper 1958). The polygons are either squares or triangles with respective proportions $p_C = 1/3$ and $p_T = 2/3$. From equation (12), we deduce that $\langle n \rangle = 9\ (4p_C + 3p_T)/5 = 6$, as required. As explained in paper I, the z lattice cells which meet at a z-vertex are numbered, if necessary, from 1 to z according to the following convention: a reference vertex is defined (figure 1(a)). The numbering at every z-vertex is obtained by rotating the reference vertex and its z incoming sides in the positive sense by the smallest angle which brings both configurations into coincidence. We number the five states as follows:

$$\begin{aligned} &S1 = (12213) \qquad S2 = (13122) \qquad S3 = (31221) \\ &S4 = (21312) \qquad S5 = (22131) \end{aligned} \tag{14}$$

and we associate the probabilities p_i ($i = 1, \ldots, 5$) with them. Defining

$$q_{ij} = p_i p_j \tag{15}$$

we calculate, for independent states,

$$\begin{aligned} \mu_2 = {} & 2p_1^2 + 4(p_2^2 + p_4^2)/3 + 28(p_3^2 + p_5^2)/3 + 4(q_{23} + q_{24} + q_{45}) + 8(q_{12} + q_{14})/3 \\ & - 4(q_{13} + q_{15})/3 + 16(q_{25} + q_{34})/3 + 16q_{35}. \end{aligned} \tag{16}$$

A microcomputer program, which constructs all possible configurations of states, has been used to calculate $P(n)$ and $m_n(1)$. Table 1 gives $P(n)$ and $m_n(1)$ for a DIES and for a distribution of independent states which favours the $n = 6$ class ($p_1, p_2 = p_3, p_4 = p_5 = 0.5(1 - p_1) - p_2, p_1 > p_2 > p_4$). Relations (12) and (13) allow us to show that $m_1(1) = 8$ and $m_{12}(1) = (24 + 24 \times 9/5)/12 = 5.6$ for the former distribution. Table 1 also gives $m_n(1)$ calculated from equation (2), where $a = a[nm_n]$ is obtained from a weighted least-square fit of the theoretical $nm_n(1)$ values while $a[m_n] = 1.177$. The values in brackets represent the range of $a[nm_n]$ obtained for two different weights, $w(n) = P(n)$

Table 1. Distribution of the number of cell sides $P(n)$ and $m_n(1)$ (theoretical and calculated from equation (2)) for $z = 5$ and (1) $p_i = 0.2$ for all i, $\mu_2 = 194/75 \approx 2.586\,67$, $a[nm_n] = 1.200$ (1.19 ± 0.01) ($a[m_n] = 1.177$); (2) $p_1 = 0.4$, $p_2 = p_3 = 0.2$, $p_4 = p_5 = 0.1$, $\mu_2 = 137/75 \approx 1.826\,67$, $a[nm_n] = 1.214$ (1.212 ± 0.003).

n	$P(n)$ (1)	$m_n(1)$ th.(1)	$m_n(1)$ calc.(1)	$P(n)$ (2)	$m_n(1)$ th.(2)	$m_n(1)$ calc.(2)
3	0.0427	8.000	8.062	0.0180	7.833	7.823
4	0.1365	7.269	7.246	0.1160	7.042	7.064
5	0.2261	6.772	6.757	0.2301	6.626	6.608
6	0.2389	6.432	6.431	0.2915	6.304	6.304
7	0.1813	6.185	6.198	0.2153	6.084	6.087
8	0.1045	6.012	6.023	0.0964	5.911	5.925
9	0.0480	5.889	5.887	0.0243	5.811	5.798
10	0.0171	5.795	5.779	0.0067	5.710	5.697
11	0.0043	5.700	5.690	0.0013	5.637	5.614
12	0.0005	5.600	5.615	0.0003	5.533	5.545

(table 1) and $w(n)=1$. A further example is $p_1=0.5$, $p_2=p_3=0.25$ for which $P(5)=0.1875$, $P(6)=0.3411$, $P(7)=0.2187$ and $a[nm_n]=1.20\pm0.04$. As for $z=4$ and $p\neq0.5$ (paper I), the theoretical $m_n(1)$ seems to oscillate around a $c+d/n$ curve which is well approximated by the Aboav-Weaire law. It is therefore likely, as in the former case, that there is no simple expression giving $m_n(1)$ as a function of n.

3.2. $z=6$

A microcomputer program constructs all the possible $(Q(6))^3=2744$ configurations of states on a triangle and calculates $P(n)$ and $m_n(1)$ for any distribution of independent states on the lattice sites.

Table 2 gives $P(n)$ and $m_n(1)$ for a DIES: a direct calculation, with $\langle i\rangle=2$, $\langle i(1,6,1)\rangle=2.8$, in fact gives $m_3(1)=2\times2.8+2=7.6$, $m_4(1)=(7.6+6.6)/2=7.1$, $m_{11}(1)=62/11\approx5.6363$ and $m_{12}(1)=(3\times8+21\times2)/12=5.5$ (see also appendix 1). Deviations from the Aboav-Weaire relation explain the large difference between $a[nm_n]=1.2414$ and $a[m_n]=0.9743$. They occur mainly for $n=3$ and $n>9$ as also observed for soap froths (Aboav 1980), for simulations of vertex models (Nakashima *et al* 1989), for the random Voronoi froth as well as for the Voronoi tessellation generated from eigenvalues of complex random matrices (Le Caër and Ho 1990). similar deviations from the Aboav-Weaire relation are also observed for non-equiprobable states, for example, when different weights are given to each of the three configurations [*141222*], [*123123*] and [*131313*].

Table 2. Distribution of the number of cell sides: *a*) $P'(n)=2744\ P(n)$ and $m_n(1)$ for $z=6$ and a DIES on a triangular lattice $p_i=1/14$ $(i=1,\ldots,14)$, $\mu_2=18/7\approx2.571\,43$. For equation (2), $a[m_n]=0.9743$.

n	$P'(n)$	$m_n(1)$ (th.)	$m_n(1)$ calc. (equation (2))
3	125	7.600	7.831
4	375	7.100	7.130
5	600	6.740	6.709
6	650	6.462	6.429
7	510	6.246	6.228
8	300	6.065	6.078
9	132	5.909	5.961
10	42	5.771	5.867
11	9	5.636	5.791
12	1	5.500	5.727

3.3. $z_1=12$, $z_2=6$, $z_3=4$

A planar tessellation by triangles whose vertices belong respectively to $z=12$, 6, 4 triangles (Coxeter 1973, p 67 and figure 4(*a*)) has also been investigated. As $Q(12)=16\,796$, $P(n)$ has only been calculated for a DIES with the help of equation (5) ($\mu_2=3.126\,37$, table 3). The most probable number of sides is now $n=5$. Using equations (12), (13) and (A1.2), we calculate $m_n(1)$ (table 3). As before, deviations from the Aboav-Weaire law occur mainly for small and large number of sides ($a[m_n]=$

Table 3. Distribution of the number of cell sides: *a*) $P'(n) = 470\,288\ P(n)$, $\mu_2 = 3.126\,37$ and $m_n(1)$ for a DIES on the vertices of a 12-6-4 tessellation ($a[m_n] = 0.7905$, $[anm_n] = 1.0507$).

n	$P'(n)$	$m_n(1)$	n	$P'(n)$	$m_n(1)$
3	24 310	7.5030	10	11 198	6.0601
4	72 930	7.0030	11	4 434	5.9457
5	104 676	6.7336	12	1 492	5.8301
6	102 674	6.5373	13	412	5.7149
7	76 791	6.3927	14	88	5.6006
8	46 761	6.2812	15	13	5.4872
9	24 508	6.1720	16	1	5.375

0.7905, $a[nm_n] = 1.0507$). For the tiling with 24-4-4 and 24-6-4 triangles in equal proportions described by Grünbaum and Shephard (1987, p 192) we calculate $P(5) = 0.2282$, $P(6) = 0.2012$, $\mu_2 = 3.753\,57$ (see also figure 7) and $m_3(1) = 7.301$ for a DIES.

3.4. z-4-4 and z-z

The $P(n)$ distributions of cellular structures associated with the two planar tessellations of figure 3, called here *z*-4-4 and *z*-*z*, may also be obtained, in the limit $z \to \infty$, from two spherical tessellations for which $\langle n \rangle_\infty = 6$. The latter consists of z half great circles which share two poles. The first tessellation moreover includes an equatorial circle.

The properties of such 'Big Bang' structures which emerge from the unfolding of structures mainly crumpled into two unstable points are also worth investigation.

3.4.1. z-4-4. The valence is (figure 3(*a*))

$$z = 8(1 + n_q) \tag{17}$$

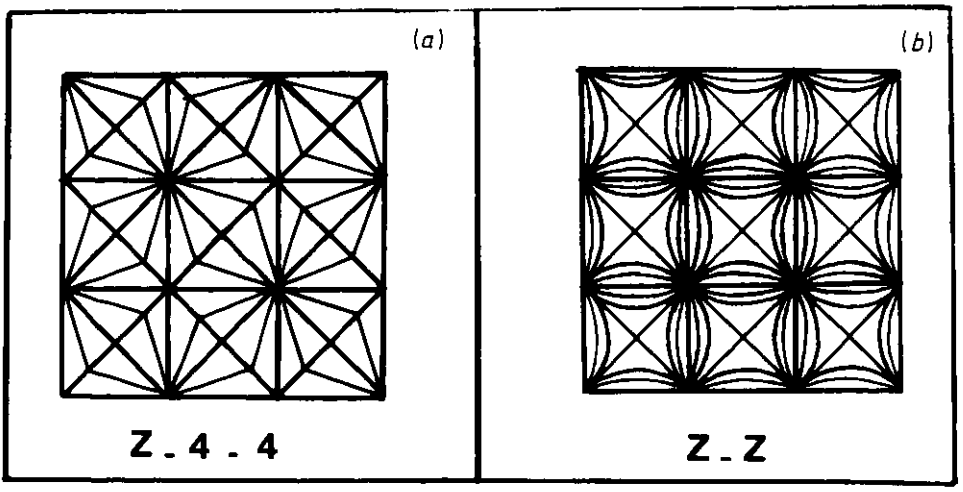

Figure 3. (*a*) *z*-4-4 tessellation for $z = 16$ (the numbering convention is given in figure 4(*b*)). (*b*) *z*-*z* tessellation for $z = 24$.

where 8 accounts for the contribution of the sides and diagonals of the square lattice and n_q is the number of remaining segments in every octant ($n_q = 1$ for figure 4(b)). As we deal only with the limit $z \to \infty$, we do not need to take into account the z-z-4 triangles (fraction $8/z$). A possible numbering convention is given in figure 4(b). Defining p as the probability of a state chosen arbitrarily among the two states (1212) and (2121), we use equation (6) to obtain

$$\begin{aligned} &R = p(1-p) \qquad P(3) = R/4 \qquad P(4) = (1-R)/4 \\ &P(n) = \{n(R+2) - 6 - 6R\}/2^{n-1} \qquad n \geqslant 5 \end{aligned} \tag{18}$$

and $\mu_2 = 4 + 2R$, for a DIES on the z-vertices, a distribution of independent states on the 4-vertices and $z \to \infty$. The maximum $P(n)$ is obtained for $n = 5$ while $P(6) = 0.1875$ *is independent of* R. For $R = 0$, $P(n)$ is simply written as

$$P(n) = (n-3)/2^{n-2}. \tag{19}$$

If we let $z \to \infty$ for the state $(1, z-2, 1, 2, \ldots, 2)$, we deduce that $m_\infty(1) = 2 + 3 = 5$, where 3 comes from the application of equation (12), valid for any distribution of states, to two tetravalent vertices. The same result holds for tilings with (z-$z1$-$z2$-. . . - etc) polygons where $z1, z2, \ldots,$ etc remain finite only while $z \to \infty$. For example, a tiling with z-6-3 triangles and 3-3-6-6 quadrilaterals ($\langle n \rangle = 6$) is easily derived from the spherical tessellation z-4-4, by erasing an arc of half of the great circles in order to replace one-half of the tetravalent vertices by two trivalent vertices. This will create 3-3-6-6 quadrilaterals while trivalent and hexavalent vertices will alternate along the equator. The same tiling is also easily constructed from figure 3(a). The derivation of the Aboav-Weaire relation also yields $m_\infty(1) = 5$ (Weaire 1974, Blanc and Mocellin 1979, Rivier 1985); it is obtained for cellular structures in statistical equilibrium under the two elementary topological transformations, neighbour switching and face disappearance. It implies that $a = 1$ in relation (2). For $R \neq 0$, $m_3(1) = 22/3 \approx 7.333$ is

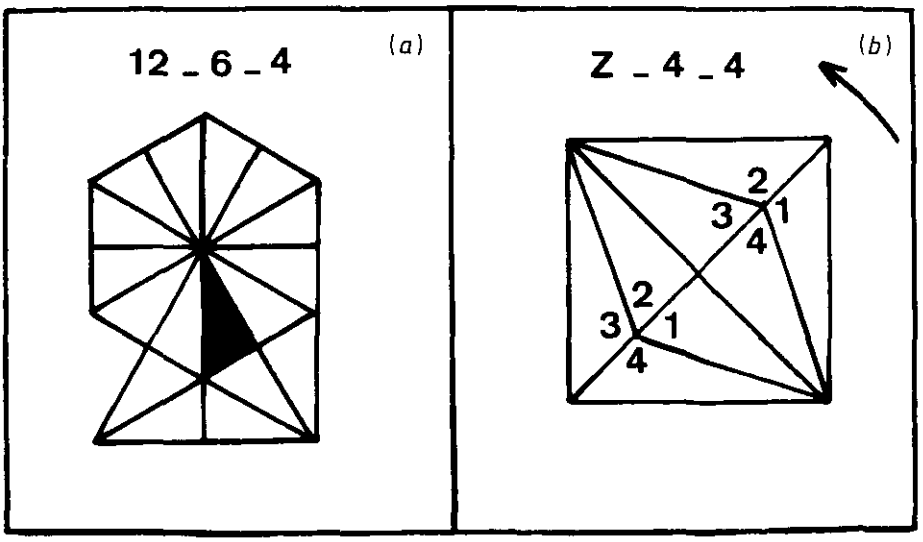

Figure 4. (a) A triangle (filled) and its 16 neighbours in a 12-6-4 tessellation. (b) The numbering convention for the 'z-4-4' tessellation of figure 4(a). One rotation of 90° in the positive sense allows us to obtain a complete numbering.

calculated with the help of relations (12) and (13) while we expect $8.333 < m_3(1) \leqslant 8.5$, according to the value of p, from relation 2 with $a = 1$.

In his statistical crystallography theory of random cellular networks, Rivier (1985) has determined the equilibrium structures using maximum entropy inference under few constraints such as space-filling, Euler's relation, correlations between cell sizes and shapes, etc. When the latter constraint is the Lewis law which relates the mean area of n-sided cells linearly to n, the resulting structure, called 'ideal' by Rivier, has

$$P(n) = \text{constant} \times (n - n_0) \exp(-cn) \tag{20}$$

with n ranging from n_1 to ∞. For $n_0 = 3$ and consequently $n_1 = 4$, the maximum entropy distribution 20 has $c = \log 2$, $\mu_2 = 4$ (appendix B of Rivier 1985) and is surprisingly given by (19) which is obtained without metric constraints. This coincidence is probably accidental and does not hold for $R \neq 0$. Figure 5 nevertheless shows that both distributions, with $\mu_2 = 4.5$, differ little for $n \geqslant 5$ when $R = 0.25$ in (18) and $n_0 \approx 2.9302$, $\exp(c) \approx 1.9403$ in (20).

3.4.2. z–z. The valence is given by relation (17) where n_q is now the number of arcs in every octant (figure 3(*b*)). The tiling consists of z–z–4 triangles (proportion $8/z$) and of z–z two-sided cells. The distribution of the number of cell sides for a DIES and $z \to \infty$ is

$$P(n) = \sum_{i=1}^{n-1} P_0(i, \infty) P_0(n - i, \infty) = n(n^2 - 1)/(24 \times 2^n) \qquad n \geqslant 2 \tag{21}$$

with $\mu_2 = 8$. We have also computed $P(n, z)$ and we compare in figure 6 $P(n, 40)$ with $P(n)$ for a 2D Johnson–Mehl froth investigated by computer simulation by Frost and Thompson (1987). This grain structure with hyperbolic grain boundaries, concave cells and lenses ($n = 2$), results from continuous nucleation with constant growth rate. Nucleation sites are implanted in space and time according to 2D and 1D Poisson point processes respectively. The distribution (21) differs little from the Johnson–Mehl distribution. From (12) and (13), $m_2(1)$ is

$$m_2(1) = 4(2z - 5)/(z - 1) + 6/(z - 8) \tag{22}$$

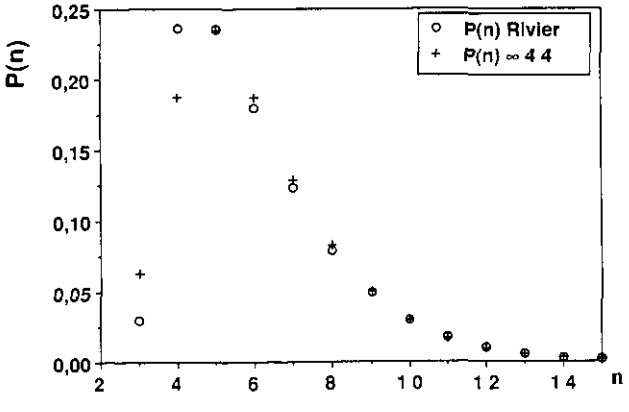

Figure 5. Distribution $P(n)$ of the number n of cell sides for a ∞–4–4 tessellation with $p = 0.5$ (crosses, equation (18)) and for the maximum entropy distribution of an 'ideal' structure (Rivier 1985) with the same $\mu_2 = 4.5$ (open circles, equation (20) with $n_0 \approx 2.9302$ and $c \approx 0.6628$).

($\approx$7.835 for $z=40$) and tends to 8 for $z\to\infty$. As $m_2(1)\approx 9.6$ for the Johnson-Mehl structure (figure 12 of Frost and Thompson 1987), we conclude that the topological properties of these two structures differ.

4. Discussion

4.1. Characteristics of the topological models for $z\geqslant 5$

For a distribution of equiprobable and independent states on the sites, the results of section 3 may be summarized as follows for $z\geqslant 5$.

(i) The distribution $P(n)$ has a maximum value which is less than 0.30 and ranges from $\approx$0.20 to $\approx$0.25. The mode is $n=6$ for the smaller valences and changes to $n=5$ when z increases.

(ii) $P(n)$ and more generally the topological properties are not strongly sensitive to the starting lattice.

(iii) μ_2 tends to increase and $m_3(1)$ tends to decrease when z increases.

(iv) For $z=5$, the Aboav-Weaire relation constitutes a very good approximation of the n dependence of $m_n(1)$, with a coefficient $a\approx 1.2$ as found in natural structures (Aboav 1980). Deviations from this relation occur mainly for $n=3$ and for $n\geqslant 9$ when $z\geqslant 6$.

The distributions $P(n)$ are typical of the distributions found experimentally for the grain structures which results from planar cuts of polycrystals (Hu 1974 (Fe), Blanc and Mocellin 1979 (alumina), Fradkov *et al* 1985 (Al), Glazier 1989, Righetti *et al* 1991 (alumina)). The experimental distribution $P(n)$ for zone-refined iron isothermally annealed at 650 °C for 125 min (Hu 1974) is, for example, compared in figure 7 with $P(n)$ calculated for a mixed (26-6-4, 26-4-4) tessellation (section 3.3). The correlations have not been determined in all the previous experiments. For alumina (Righetti *et al* 1991), $a[m_n]=1.12$, 1.07 and $a[nm_n]=0.94$, 0.99 for weights 1 and $P(n)$ respectively.

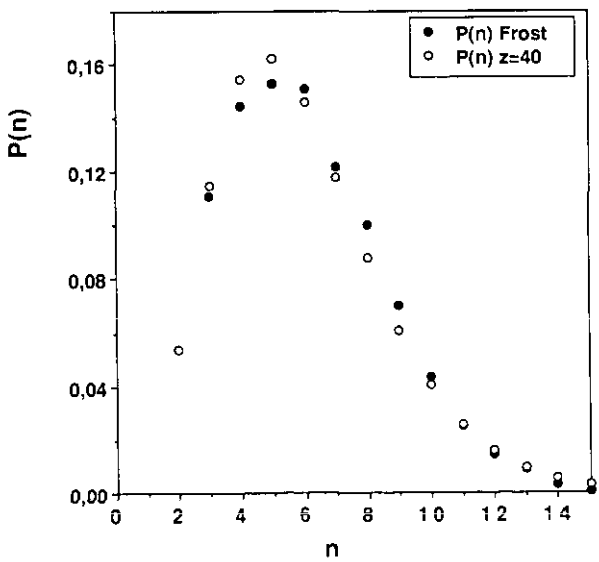

Figure 6. Distribution $P(n)$ of the number of cell sides for a z-z tessellation with $z=40$ (open circles) and simulated distribution for a 2D Johnson-Mehl froth (full circles) (Frost and Thompson 1987).

The $m_n(1)$ values for the domain structure in this films of glassy As_2Se_3 (Chen *et al* 1984, see figure 3 of paper I for $P(n)$) are $\approx$7.03, 6.59, 6.33, 6.07, 5.95 and 5.80 for n ranging from 4 to 9. The latter $m_n(1)$ are strikingly close to the values given in table 1 for distribution no. 2. For a DIES, the results differ, whatever the considered lattice, from the experimental observations for soap froths (Glazier *et al* 1990) with, for example, $P(5)=0.314$ and $P(6)=0.305$.

The $P(n)$ of section 3 are also quite similar to the $P(n)$ yielded by various structural models of polycrystalline grain growth (see Atkinson 1988 for a recent overview with a classification of models and Glazier *et al* 1990 for a compilation of typical $P(n)$ distributions). The side-cell distributions for one of the two maximum configuration entropy models of Kikuchi (1956, Glazier *et al* 1990) and for a DIES on a $z=5$ lattice are almost identical. Moreover, the distributions of section 3 do not differ crucially (figure 8(*a*)) from the distributions derived from vertex models which are based on equations of motion for vertices (Soares *et al* 1985, Nakashima *et al* 1989) or from a Potts model, with nearest-neighbour ferromagnetic interactions, on a triangular lattice at $T=0$ (Sahni *et al* 1983).

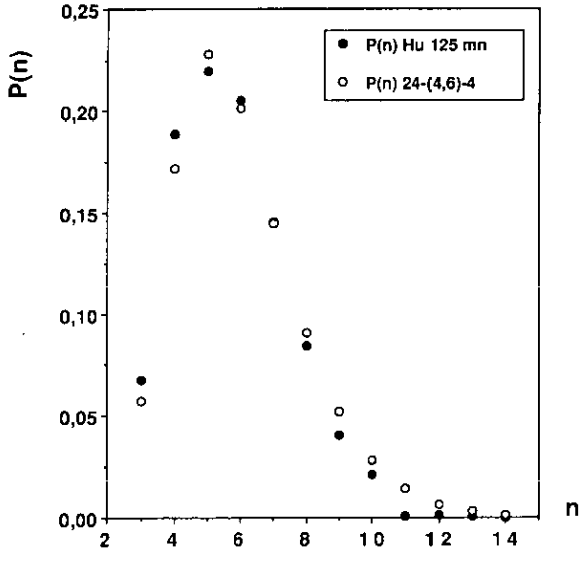

Figure 7. Distributions $P(n)$ of the number n of cell sides for zone-refined iron isothermally annealed at 650 °C for 125 mn (full circles, Hu 1974) and for a DIES on the vertices of a 26-6-4, 26-4-4 tiling (open circles).

4.2. The relation between the topological defect concentration C and μ_2

Carnal and Mocellin (1981) have investigated the conditions which must be fulfilled by the distributions $P(n)$ in random plane sections of polycrystals evolving by the two elementary 2D topological transformations (neighbour switching and face disappearance, Weaire and Rivier 1984, paper I) in order to remain invariant during grain growth. The variance of $P(n)$, μ_2 and the topological defect concentration C

$$C=\left\{\sum_{n\geqslant 3}|n-6|P(n)\right\}\Big/2=3P(3)+2P(4)+P(5) \tag{23}$$

are not independent in their model. We show in figure 8(*b*) the very regular behaviour of $C(\mu_2)$ for the topological models when z increases from 4 to ∞. For $z=4$ ($0 \leqslant \mu_2 \leqslant 1$) and for independent states (paper I)

$$C = (4\mu_2 - \mu_2^2)/8. \tag{24}$$

This relation also describes quite accurately the results obtained for states correlated on a square lattice according to a nearest-neighbour ferromagnetic ising model (paper I, Delannay *et al* 1991).

We present in figure 8(*b*) (C, μ_2) points calculated from the distributions $P(n)$ of a number of cellular structures. There is a clear clustering of all points in a narrow region of the (C, μ_2) plane. Such a clustering seems significant. It is indeed easy to construct artificial distributions $P(n)$ with completely different $C(\mu_2)$ relations; for instance, the distributions $P(m) = P(12-m) = p$, $P(6) = 1-2p$ ($m = 3, 4, 5$) have $C = \mu_2/\{2(6-m)\}$ ($0 \leqslant \mu_2 \leqslant (6-m)^2$). The observed clustering probably results from general features, not related to the actual values of $P(n)$, as the topological models (and the maximum entropy model, see below) do not account for the $P(n)$ of all structures (section 4.2). Only a rather narrow range of C values may be available for 'reasonable' structures as a consequence of $\langle n \rangle = 6$ and of $n \geqslant 3$ for a given μ_2 in the range 0 to ~3. By 'reasonable', we mean for instance structures with 'smooth', 'unimodal' $P(n)$ although these characteristics have to be worked out when applied to discrete distributions. We have calculated the distributions $P(n)$ which are deduced from the application of the maximum entropy (S) principle ($S = -\Sigma P(n) \log P(n)$, Jaynes 1957, Rivier 1985, Maxent on figure 8(*b*)) with the sole constraints $\langle n \rangle = 6$ and $\langle (n-6)^2 \rangle = \mu_2$ for n ranging from 3 to ∞. The maximum entropy distributions tend to be smooth because they tend to have the most nearly uniform distribution satisfying the given information (Brand and Le Caër 1988 and references therein). Figure 8(*b*) confirms that the corresponding $C(\mu_2)$, although different, is very close to $C(\mu_2)$ 'topological' for $\mu_2 \leqslant 2.5$ while C is larger for the maximum entropy distribution for $\mu_2 \geqslant 2.5$. The Carnal-Mocellin $C(\mu_2)$ curve ($\mu_2 \geqslant 2.5$) is located between the two previous curves. For $\mu_2 \geqslant 3.5$, the experimental values are satisfyingly accounted for by the 'topological' $C(\mu_2)$ line. It is worth mentioning that, for $\mu_2 \leqslant 1$, the maximum entropy distributions $P(n)$ are very similar to the $P(n)$ calculated both for independent and for correlated distributions of states [1212] on a square lattice ($z = 4$, paper I, Delannay *et al* 1991) as well as to the $P(n)$ observed in some biological tissues (Glazier 1989, table 2 in paper I). The previous structures differ mainly in the intercell correlation $(m_n(i), i = 1, \ldots)$. The $P(n)$ differ more and more when z increases: $P(5) > P(6)$ for $\mu_2 \geqslant 4.1$ for the maximum entropy distributions while this happens for smaller values of μ_2 (~3) for the topological models (table 3).

4.3. Some hints about possible connections between the models and actual structures

The problem of the reverse transformation from a cellular structure to a lattice with unstable sites is therefore raised. Although we have not solved that problem, we argue below that we do not need actually to perform unphysical and improbable collapses of many vertices (>4) into one in order to use the present models. We 'only' need to describe the structure as a forest, that is, a disconnected graph whose components are all trees (Essam and Fisher 1970), and further to connect the trees by bonds which close the existing cells. The latter bonds are the sides of the unconditional neighbours (section 3) and they determine the topology of the sought-after tessellation. The group

of grains of figure 9(*a*) or (*b*) may, for example, be described as a juxtaposition of a $z=7$ state and of other states which will depend on the grains which are at the border of this group. Secondly, figure 9 shows that a local neighbour switching (T1) which transforms the group of grains of (*a*) into the group of (*b*) may be interpreted as a state 'flipping' at a $z=7$ vertex. The proposed description is not unique and states from coordination numbers ranging from 4 to >7 may be used as well. A given structure

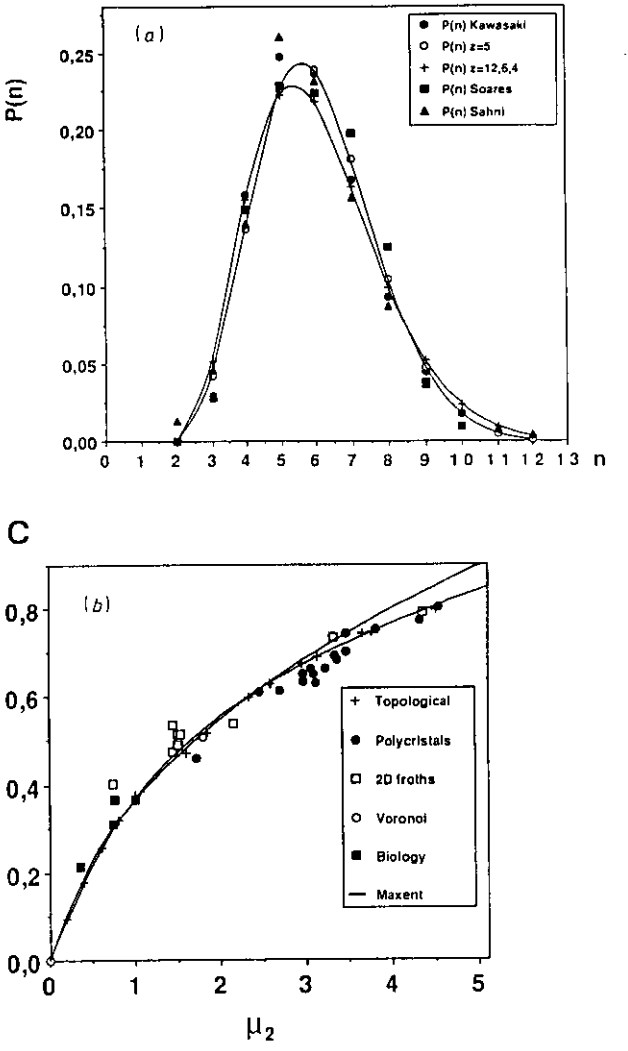

Figure 8. (*a*) Distributions $P(n)$ of the number n of cell sides for vertex models (full circles, Kawasaki *et al* 1989, full squares, Soares *et al* 1985), for a Potts model on a triangular lattice (full triangles, Sahni *et al* 1983) and for a DIES on $z=5$ and $z=12$-6-4 (figure 4(*a*)) tessellations (full lines). (*b*) Topological defect concentration C (equation (23)) as a function of μ_2 for various 2D cellular structures (crosses and associated full line, topological models for $z=4$ to ∞; full circles, polycrystal cuts (Glazier 1989, Righetti *et al* 1991*b*); open squares, various 2D soap froths, lipid monolayers (Glazier 1989); open circle, random Voronoi froth (Le Caër and Ho 1990); full squares, biological tissues (Glazier 1989, paper I); full line (upper line for $\mu_2 \geqslant 3$), maximum entropy distribution).

can be described as a juxtaposition of states arising from different valences. Among all the arrangements, some may possibly be mapped on a tiling topologically closer to a 'regular' tessellation with a limited number of valences than to a random tessellation, as further the topological properties change slowly with z. Moreover local T1 transformations may take place without significantly changing the valence distribution. With this type of 'molecular' description, we may even envisage accounting for structures without knowing by which actual transformations they have been produced. How to determine the effective z and the interactions between states for an actual given structure remain unanswered questions. For cellular structures evolving mainly by neighbour-switching transformations (i.e. monolayers of pentadecanoic acid, Stine *et al* 1990), the average effective valence may be inversely related to the rate of these processes.

We conclude that the present models, with a DIES on the lattice sites, give a realistic description of the topological properties of the cellular networks of polycrystal cuts. Correlations among the states must be considered in order to know whether or not the models are able to describe the topological properties of soap froths. The method may be used, by including some simple metric rules, to produce initial structures for dynamical studies.

5. Conclusion

Our aims in the construction of controlled models of random cellular networks, described in a previous paper and in the present work, have been primarily to perform exact calculations of their topological properties in order to compare them with existing models. We have deliberately postponed the introduction of physical constraints in the models as they may hide the actual origin of some characteristics of the structures investigated. To our surprise, the models give an acceptable description of the topological properties of some natural or simulated cellular structures. Although we feel the necessity for deeper explanations, we do not need to put forward unrealistic physical mechanisms in order to understand this reasonable agreement if the structure can be described as a juxtaposition of states constituting a sufficiently regular forest. The structures generated for $z \geqslant 5$ from a distribution of equiprobable and independent states are characterized by a reduced variability of their topological properties whatever the subject 'mother' lattice. The existence of a lattice and of interactions among the states, which would give rise to a distribution $P(n)$ given beforehand, is therefore not guaranteed. The description of soap froths has not been reached and distributions of interacting states on the sites of various lattices will have to be investigated for that purpose.

Acknowledgments

I wish to thank R Delannay, D Fraser, T Liebling and A Mocellin for useful discussions.

Appendix 1

The components of the states must, at least, satisfy the following constraints.

(i) At least two components equal to 1 (at least two ends).

(ii) No two successive 1 (valence = 3 in the final structure).

(iii) No 121 or 212 sequences for $z > 4$ (the graph is connected, see also equation (A2.3)).

(iv) As $n_1(j|i, 3) \neq 0$ (equation (7)) only if $z - 1 \geqslant i + j$, the sum of two successive components must be less than z.

Besides the $[1, z-2, 1 \ldots 2]$ configuration, there is another configuration which can be simply constructed.

(i) If z is even, it consists of two identical groups $[1, 2, 3 \ldots 3, 1, 2, 3 \ldots 3]$ with, as a whole, two values of 1, two values of 2 and $z-4$ of 3.

(ii) If z is odd, it is $[1, 2, 3 \ldots 3, 2, 1, 3 \ldots 3]$ with two values of 1, two of 2, $z-4$ of 3 divided in two groups: one $(123 \ldots 32)$ with $[z/2]-2$ and one $(13 \ldots 3)$ with $[z/2]-1$ values of 3 (ex: $z = 7$, [1232133]).

The state components can be simply obtained from Euler's triangulation of a convex polygon with z sides by non-intersecting diagonals (Gardner 1976, Cohen 1978): $S_{kj} - 1$ is the number of diagonals at the jth vertex of the subject polygon (figure 10(a)).

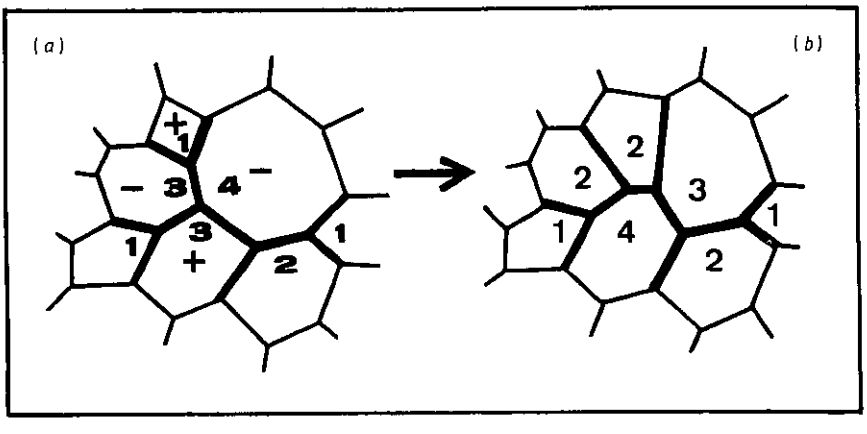

Figure 9. Neighbour switching (+ and −) in a group of cells in (a) which transforms it into the group of (b). This transformation may, for example, be interpreted as a state 'flipping' from (1313214) to (2214231) (bold lines) on a $z = 7$ vertex.

In the following, the state components from 1 to z are written on the vertices of a convex z-polygon. At a given lattice site the cell associated with the jth sector ($j = 1, \ldots, z$), has:

(i) two unconditional neighbours ($j \pm 1$) whose state components are $S_{kj\pm1}$;

(ii) $S_{kj} - 1$ conditional neighbours.

Two components S_{kj} and S_{kl} are conditional neighbours if the vertices j and l of the previous z-polygon are joined by a diagonal (jl-diagonal). Neighbour switching, which involves four state components S_{ki}, S_{kj}, S_{kl} and S_{km} with, for example, cells j and l sharing an added side, is simply performed by erasing the jl-diagonal and drawing the im-diagonal.

Except for small valences or for the $(1, z-2, 1, 2 \ldots 2)$ state, it is not obvious to find the conditional neighbours among the components of any state. With any state, we associate a $z \times z$ neighbour matrix N whose elements are $N(l, m) = N(m, l) = 1$ if cells m and l ($m, l = 1, \ldots, z$, $m \neq l$) share an added side in the stable arrangement. A 'pruning' algorithm allows us to calculate the elements of N. It is based on the fact

that the two nearest non-zero components on both sides of a component $S_{kl}=1$, S_{kl} and S_{km} share an added side. If the corresponding branch is cut away from the state under consideration, that is S_{kl} and S_{km} are decreased by 1 and S_{kj} is set to zero, the remaining graph is still a state with $z^* \leqslant z-2$ and at least two components equal to 1. The procedure can therefore be iterated until only a $z^*=4$ or a $z^*=3$ state is left. At every step, all the components equal to 1 are set to zero, all their non-zero neighbours are decreased by 1 and the corresponding elements of N are set to 1. The sum of the elements of any N matrix is $2z-6$. At most $[(z-3)/2]$ lines ($z>4$), not including the last one with $z^*=4$ or $z^*=3$, are needed to write these steps. For example, the pruning algorithm applied to the $z=14$ state of figure 2(a) gives:

	$j=1$	2	3	4	5	6	7	8	9	10	11	12	13	14	
Step 1	1	4	3	1	4	2	2	2	2	1	6	4	2	2	$N(2,14)=N(3,5)=N(9,11)=1$
Step 2	0	3	2	0	3	2	2	2	1	0	5	4	2	1	$N(8,11)=N(2,13)=1$, $z^*=11$
Step 3	0	2	2	0	3	2	2	1	0	0	4	4	1	0	$N(7,11)=N(12,2)=1$, $z^*=9$
Step 4	0	1	2	0	3	2	1	0	0	0	3	3	0	0	$N(3,12)=N(6,11)=1$, $z^*=7$
Step 5	0	0	1	0	3	1	0	0	0	0	2	2	0	0	$N(5,11)=N(5,12)=1$, $z^*=5$
Step 6	0	0	0	0	1	0	0	0	0	0	1	1	0	0	STOP $z^*=3$.

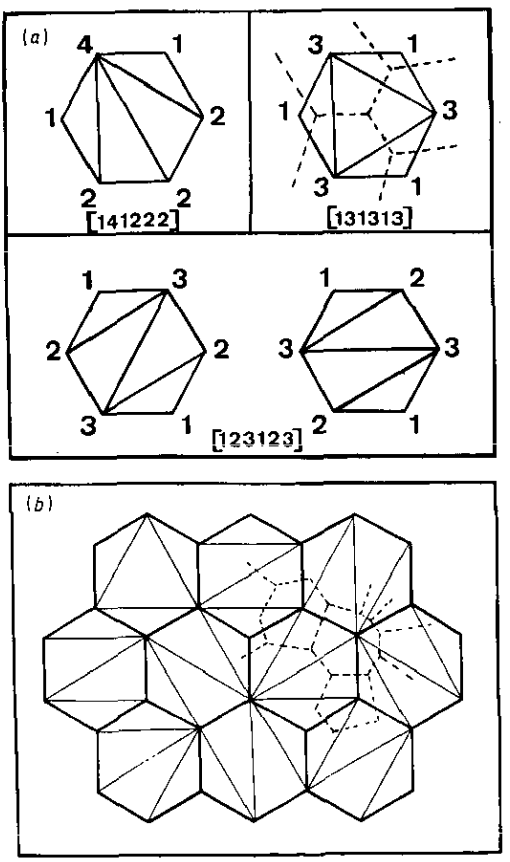

Figure 10. (a) The relation between Euler's polygon triangulation and some states for the case $z=6$ (see also Gardner 1976 and Cohen 1978). (b) The diagonal triangulation method on the honeycomb lattice for $z=6$ and some cells of the associated cellular structure (broken lines).

At a z-vertex, the contribution of sector number j to the total number of sides of the neighbouring cells of the associated n-cell is

$$V_{kj} = S_{kj-1} + S_{kj+1} + \sum_{m=1}^{z} S_{km} N(m, j). \tag{A1.1}$$

For a DIES and for a fixed value $S_{kj} = i$, the average $\langle V_{kj} \rangle$ allows us to calculate $m_n(1)$:

$$\langle V_{kj} \rangle = 2i \operatorname{av}(i, z, 1) = 2(i+1)(2z-i-4)/(z-1). \tag{A1.2}$$

Euler's diagonal triangulation can be used to define an equivalent method of construction of the cellular structure. Every polygon of the dual lattice L^* of the unstable lattice L is triangulated (T) by non-intersecting diagonals. L^* is thus transformed into TL^* whose dual CL is the associated cellular structure (figure 10). A cell is associated with every vertex of L^*. Its number of sides is equal to the sum of the state components or to the total number of sides and of diagonals which merge in that vertex. Figure 10(b) shows an example, for $z = 6$, with a triangulation of the honeycomb lattice. Extensions of the method include, for instance:

(i) triangle creation or annihilation, performed by triangulating (at most once) already existing triangles of TL^* or by deleting the vertex and the three sides included in a triangle of TL^* respectively, before constructing CL;

(ii) topological models of 3D cellular structures using tetrahedra.

The TL^* construction may finally be useful for defining metric rules for CL and for producing computer images of such cellular structures.

Appendix 2

The variances of the distributions $P_0(i, z)$ and $P_1(j|i, z)$ are, respectively:

$$\operatorname{var}(z, 0) = 2(z-2)(z-3)(2z-3)/\{z^2(z+1)\} \tag{A2.1}$$

$$\operatorname{var}(j, z, 1) = (z-2-j)[2z^2(j^2+3j-2) - z(j^3+11j^2+22j-8) + 2j(j+3)(j+4)]/\{j^2 z(z-1)^2\}. \tag{A2.2}$$

Using the method described in section 2, we derive the distribution $P(j|k|i, z)$ which is the probability of observing a sequence of components $(jki\ldots)$ for equiprobable states on a z-vertex and for a given k in a fixed position among the z possible ones (the result is obviously independent of that position). $P(j|k|i, z)$ allows us to calculate $P_2(j|i, z)$.

$$n(j|k|i, z) = \{(i+j+K-4)/(z-4)\} C^{z-5}_{2z+5-i-j-K} \tag{A2.3}$$

and

$$K = k(1-\partial_{k1}) \qquad z-2 \geqslant i, j \geqslant 1 \qquad \text{except } j \geqslant 2 \text{ if } k = 1 \tag{A2.4}$$

where ∂_{k1} is the Kronecker symbol. Using equation (4), we finally write

$$P(j|k|i, z) = n(j|k|i, z)/n(k, z). \tag{A2.5}$$

As

$$P_1(k|i, z) = \sum_{j=1}^{z-2} P(j|k|i, z) \tag{A2.6}$$

the average of $P(j|k|i, z)$ is $\langle i\rangle = \langle j\rangle = \mathrm{av}(k, z, 1)$ (equation 13) and its variance is $\langle (i-\langle i\rangle)^2\rangle = \langle (j-\langle j\rangle)^2\rangle = \mathrm{var}(k, z, 1)$ (equation A2.2). The covariance of the distribution (A2.5) is $\mathrm{cov}(k, z) = \langle (j-\langle j\rangle)(i-\langle i\rangle)\rangle$:

$$\mathrm{cov}(k, z) = -(2z-4-k)(z-2-k)(2z+k[k+3])/\{k^2 z(z-1)^2\} \qquad \text{(A2.7)}$$

for $z-2 \geqslant k \geqslant 2$ and

$$\mathrm{cov}(1, z) = -(z-4)(z-3)(z+5)/\{z(z-1)^2\}. \qquad \text{(A2.8)}$$

Summing $n(j|k|i, z)$ over k and dividing by $n(j, z)$ allows us to obtain

$$P_2(j|i, z) = P_1(j|i+1, z) + \{(j-1)/j\}[(z-2)/(2z-5-j)]P_1(j-1|i-1, z-1) \qquad \text{(A2.9)}$$

with $P_2(1|i, z) = P_1(1|i+1, z) = P_0(i, z-1)$ as given in section 2. The average of $P_2(j|i, z)$ is

$$\langle i(j, z, 2)\rangle = \mathrm{av}(j, z, 2)$$
$$= [(j+1)/j]\{(2z-j-4)/(z-1)\} - \partial_{j1} + [(j-1)/j]\}(z-2)/(2z-5-j)\}. \qquad \text{(A2.10)}$$

The random variable $nm(n, 1)$ is the total number of sides of the first-neighbour cells of an n-cell and its average is $nm_n(1)$. The previous relations can be used to calculate the standard deviation $\mathrm{sd}_m(3)$ of the distribution of $m(3, 1)$ for various tessellations and for a DIES:

$$\mathrm{sd}_m(3) = [\mathrm{var}(4, 0) + \mathrm{var}(6, 0) + \mathrm{var}(12, 0) + 2\,\mathrm{var}(1, 12, 1) + 2\,\mathrm{var}(1, 6, 1)$$
$$+ 2\,\mathrm{cov}(1, 12) + 2\,\mathrm{cov}(1, 6)]^{1/2}/3 \approx 0.7781$$

for the 12-6-4 tessellation (figure 3(a)) and

$$\mathrm{sd}_m(3) = (2\,\mathrm{var}(4, 0) + \mathrm{var}(\infty, 0) + 2\,\mathrm{var}(1, \infty, 1) + 2\,\mathrm{cov}(1, \infty))^{1/2}/3$$
$$= (7/6)^{1/2} \approx 1.0801$$

for the z-4-4 case (figure 3(a)) when $z \to \infty$.

References

Aboav D A 1970 *Metallography* **3** 383-90
—— 1980 *Metallography* **13** 43-58
Almgren F J Jr and Taylor J E 1976 *Scientific American* **235** (July) 82-93
Atkinson H V 1988 *Acta Metall.* **36** 469-91
Babcock K L, Seshadri R and Westervelt R M 1990 *Phys. Rev.* A **41** 1952-62
Berge C 1970 *Graphes et Hypergraphes* (Paris: Dunod)
Blanc M and Mocellin A 1979 *Acta Metall.* **27** 1231-7
Brand R A and Le Caër G 1988 *Nucl. Instrum Methods* B **34** 272-84
Carnal E and Mocellin A 1981 *Acta Metall.* **29** 135-43
Chen C H, Philips J C, Bridenbaugh P M and Aboav D A 1984 *J. Non-Crystall. Solids* **65** 1-28
Cohen D I A 1978 *Basic Techniques of Combinatorial Theory* (New York: Wiley)
Coxeter H S M 1973 *Regular Polytopes* (New York: Dover)
Delannay R, Le Caër G and Khatun M 1991 in preparation
Essam J W and Fisher M E 1970 *Rev. Mod. Phys.* **42** 272-88
Feller W 1957 *An Introduction to Probability Theory and its Applications* vol 1 (New York: Wiley)
Fradkov V E, Kravchenko A S and Shvindlerman L S 1985 *Scripta Metall.* **19** 1291-6
Frank F C and Kasper J S 1958 *Acta Cryst.* **11** 184-90
Fraser D P 1991 *Materials Characterization* in press

Frost H J and Thompson C V 1987 *Acta Metall.* **35** 529–40
Gardner M 1976 *Scientific American* **235** (June) 120–25
Glazier J A 1989 *PhD thesis* the University of Chicago
Glazier J A, Anderson M P and Grest G S 1990 *Phil. Mag.* B **62** 615–45
Grünbaum B and Shephard G C 1987 *Tilings and Patterns* (New York: Freeman)
Hu H 1974 *Canadian Metallurgical Quarterly* **13** 275–86
Jaynes E T 1957 *Phys. Rev.* **106** 620–30
Kawasaki K, Nagai T and Nakashima K 1989 *Phil. Mag.* B **60** 399–421
Kikuchi R 1956 *J. Chem. Phys.* **24** 861–7
Knuth D E 1973 *The Art of Computer Programming* vol 1, 2nd edn (Addison-Wesley: Reading, MA)
Le Caër G and Ho J S 1990 *J. Phys. A: Math. Gen.* **23** 3279–95
Le Caër G 1991 *J. Phys. A: Math. Gen.* **24** 1307–17, 2677
Moon J W 1980 *Annals of Discrete Mathematics* **8** 117–21
Nakashima K, Nagai T and Kawasaki K 1989 *J. Stat. Phys.* **57** 759–87
Righetti F, Liebling T M, Le Caër G and Mocellin A 1991a in preparation
—— 1991b *Proc. Int. Conf. on Grain Growth in Polycrystalline Materials (Rome June 1991)* to be published
Rivier N 1985 *Phil. Mag.* B **52** 795–819
Sahni P S, Srolovitz D J, Grest G S, Anderson M P and Safran S A 1983 *Phys. Rev.* B **28** 2705–16
Shreve R L 1966 *J. Geology* **74** 17–37
—— 1967 *J. Geology* **75** 178–86
Soares A, Ferro A C and Fortes M A 1985 *Scripta Metall.* **19** 1491–6
Stine K J, Rauseo S A, Moore B G, Wise J A and Kobler C M 1990 *Phys. Rev.* A **41** 6884–92
Thompson D'AW 1917 *On Growth and Form* (Cambridge: Cambridge University Press)
Vannimenus J and Viennot X G 1989 *J. Stat. Phys.* **54** 1529–38
Viennot X G 1990 Trees everywhere *Proc. CAAP'90* Copenhagen May 1990 *(Lecture Notes in Computer Science)* in press
Weaire D 1974 *Metallography* **7** 157–60
Weaire D and Rivier N 1984 *Contemp. Phys.* **25** 59–99